

# Local Molecular Mobility as a Crucial Factor Affecting Gas Permeability of Poly(oxyethylene)s with (Alkylsulfonyl)methyl Side Chains

Seung-Yeop Kwak<sup>\*,†</sup> and Jong-Chan Lee<sup>‡</sup>

Hyperstructured Organic Materials Research Center (HOMRC), and Department of Fiber and Polymer Science, Seoul National University, San 56-1, Shinlim-dong, Kwanak-ku, Seoul 151-744, Korea, and Hyperstructured Organic Materials Research Center (HOMRC), and School of Chemical Engineering, Seoul National University, San 56-1, Shinlim-dong, Kwanak-ku, Seoul 151-744, Korea

Received August 19, 1999; Revised Manuscript Received February 21, 2000

**ABSTRACT:** Local molecular motions of four homologous series of poly[oxy(alkylsulfonyl)ethylene]s such as poly[oxy(ethylsulfonylmethyl)ethylene], poly[oxy(propylsulfonylmethyl)ethylene], poly[oxy(butylsulfonylmethyl)ethylene], and poly[oxy(pentylsulfonylmethyl)ethylene] were correlated with their oxygen permeability in conjunction with their side chains varying from ethyl, *n*-propyl, *n*-butyl, to *n*-pentyl. To characterize and evaluate the local molecular motions, measurements of proton rotating-frame spin-lattice relaxation time,  $T_{1\rho}$ , over the temperature range 140–400 K were made. Then, the corresponding correlation times,  $\tau_c$ 's, were determined from fitting the relaxation data, and the activation energies,  $E_a$ , obeying the Arrhenius relation with  $\tau_c$ , were accordingly obtained. The results of  $\tau_c$  and  $E_a$  for the poly(oxyethylene)s were consistent with their oxygen permeability coefficient where the slower local motion due to the shorter side chains imparted a lower oxygen permeability as in poly[oxy(ethylsulfonylmethyl)ethylene] and vice versa as in poly[oxy(pentylsulfonylmethyl)ethylene]. This was attributed to the fact that the longer side chains as in poly[oxy(pentylsulfonylmethyl)ethylene] pushed the neighboring chains further apart and decreased the restriction to the backbone chain motions, making them more locally mobile. This faster local motion in turn resulted in the higher oxygen permeation, while the slower local motion resulted in the higher barrier nature. The local molecular mobility evaluated by  $\tau_c$  and  $E_a$  was found to be another crucial factor governing the gas permeability of poly(oxyethylene)s.

## Introduction

Over the past decade, extensive studies have attempted to correlate various polymer characteristics with gas transport properties (permeability) in polymeric gas separation membranes or barrier polymers.<sup>1–5</sup> Most polymer characteristics affecting gas permeability generally belong to two parameters. They involve (a) structural parameters such as chain rigidity, interchain packing with *d*-spacing and fractional free volume (FFV), polarity in both backbone chains and side groups, orientation and order, etc., and (b) molecular mobility of backbone and side chains as usually determined by the sub- $T_g$  transition behavior. Concerning the former, considerable data exist and a general conclusion on the structure–permeability interrelationship has been drawn, unifying it to the extent possible. Recognizing that molecular mobility is inevitably interdependent with structure, it is also expected to be in good correlation with permeability. The molecular motion can be analyzed primarily by three relaxation techniques:<sup>6,7</sup> dynamic mechanical relaxation, dielectric relaxation, and nuclear magnetic resonance (NMR) relaxation. Dynamic mechanical relaxation measures the whole complex of intermolecular interactions that contribute to the segmental motion and hence the macroscopic modulus. Many of the studies conducted on the correlation of the molecular motion to permeability have been performed by dynamic mechanical relaxation and analysis of sub-

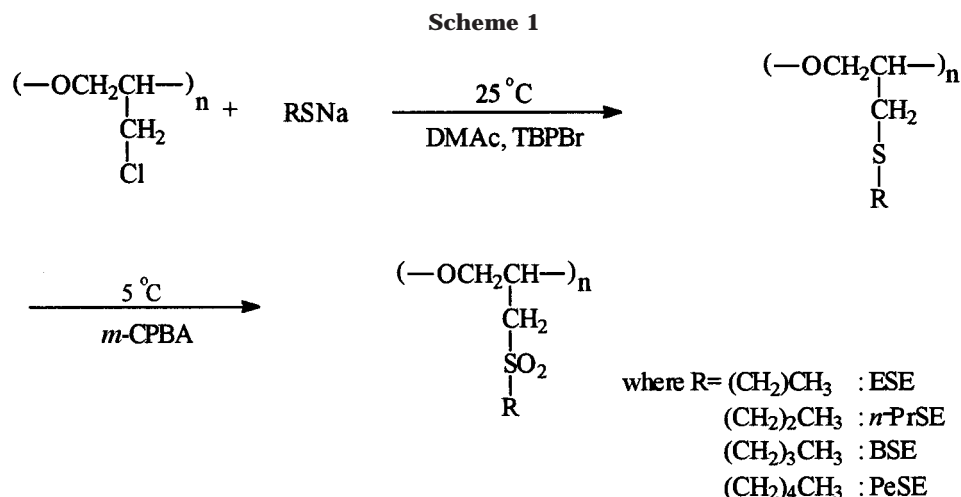
$T_g$  transition.<sup>1–5</sup> Dielectric relaxation is limited to detecting mobility only for the electric dipole of the chemical bonds in the backbone. NMR relaxation reflects the modulation events of magnetic dipoles, which are of a local scale (say less than 2–3 carbons) and of several orders of magnitude shorter than for the dynamic mechanical relaxation. Considering that the segmental motion is to be large and slow enough to affect efficiently the passage of gas molecules through the existing space between neighboring chains and the sub- $T_g$  transitions ( $\beta$ - or  $\gamma$ -transition) does not indicate the direct, quantitative measure of mobility, but an onset of side group motion;<sup>8</sup> the characterization on local chain motion by NMR is more realistic and promising for correlating with the permeability. Furthermore, it is noteworthy that since the “mobility” is often defined by the rate of motion and is a relative term, the mobility difference among the given polymers must be compared on the quantitative basis at the same temperature (particularly, at the temperature measuring the gas permeance) to distinguish and relate the mobilities to the gas permeabilities.

NMR relaxation analysis can reveal details of the local molecular motion, and indeed any discrimination of regions (i.e., main chain and side group) within a solid polymer is by employing with either pulsed wide line for <sup>1</sup>H or cross-polarization/magic angle spinning (CP/MAS)<sup>9,10</sup> for <sup>13</sup>C. The former can provide a convenient way to get information about average local motion in a whole polymeric system.<sup>11</sup> This is done by usually measuring <sup>1</sup>H spin-lattice relaxation times in the rotating frame,  $T_{1\rho}$ , for the solid polymers and eventually determining the correlation time,  $\tau_c$ , based on Bloembergen–Purcell–Pound (BPP) theory.<sup>12</sup> The correlation time,  $\tau_c$ , is defined as the average time required

<sup>†</sup> HOMRC and Department of Fiber and Polymer Science, Seoul National University.

<sup>‡</sup> HOMRC and School of Chemical Engineering, Seoul National University.

\* To whom correspondence should be addressed at School of Materials Science and Engineering, Seoul National University, San 56-1, Shinlim-dong, Kwanak-ku, Seoul 151-744, Korea.



for motional events and commonly expresses the molecular mobility of polymers. BPP theory represents a decrease in  $\tau_c$  as the motion gets faster and, hence, the mobility increases. The latter high-resolution solid-state NMR observes the <sup>13</sup>C chemical shifts and then can separate the mobility of side chains from that of the main chains. However, it must be noticed that such fast-rotating side groups as  $\alpha$ -methyl or non-hydrogenated groups follow the relaxation mechanism, not by dipole-dipole interaction (the most usual mechanism for polymers) but by other means such as spin rotation, which results in a further complexity in determining the  $\tau_c$ .<sup>13</sup>

In recently published articles,<sup>14,15</sup> excellent barrier properties for (alkylsulfonyl)methyl-substituted poly(oxyethylene)s have been reported, and chemical structure-thermal property-gas permeability relationships have been discussed; however, only limited correlations were made. The present paper extends the previous studies to investigate the effect of the local molecular motion (instead of segmental motion) revealed by <sup>1</sup>H solid-state NMR spectroscopy on gas permeability for the poly(oxyethylene)s possessing homologous (alkylsulfonyl)methyl side chains. The structural variation is different in the length of (alkylsulfonyl)methyl side chains. The central purpose of this study is to exploit systematically the potentials of NMR spin-lattice relaxation and local molecular mobility as another important parameter in governing the gas permeability of poly(oxyethylene)s in conjunction with their structural variants.

## Experimental Section

**Materials.** (Alkylsulfonyl)methyl side-chain poly(oxyethylene)s were synthesized by a two-step reaction in Scheme 1. (Alkylthio)methyl-substituted poly(oxyethylene)s were prepared by the reaction of chloromethyl-substituted poly(oxyethylene)s with sodium alkanethiolate. The starting polymer was poly[oxy(chloromethyl)ethylene] (Hydrin H). The thioether group was then oxidized using *m*-chloroperbenzoic acid (*m*-CPBA). Scheme 1 summarizes the synthetic routes and the acronyms for the resulting products: poly[oxy(ethylsulfonylmethyl)ethylene] (ESE), poly[oxy(propylsulfonylmethyl)ethylene] (*n*-PrSE), poly[oxy(butylsulfonylmethyl)ethylene] (BSE), and poly[oxy(pentylsulfonylmethyl)ethylene] (PeSE). Synthesis details were given in the previous article.<sup>15</sup>

**Permeability Measurements.** The oxygen permeability measurements were conducted using the ASTM D1434 volumetric method.<sup>16,17</sup> The volume of the atmospheric pressure side of the permeability cell is very sensitive to changes in temperature and barometric pressure. When the permeability

of a polymer is very low and measurements must be made over several days, this becomes very important. The permeability cell with a connected graduated capillary column was immersed in a constant temperature water bath at 30 °C. The temperature variation of the water bath was less than 0.002 °C. A graduated capillary tube with 0.002 05 cm<sup>2</sup> internal cross-sectional area was used to measure the volume change in the downstream side. The indicating liquid was Victoria Blue B in 4-methyl-2-pentanone. The downstream side was closed except to the capillary tube.

The volume changes due to changing barometric pressure were then measured. When the barometric pressure decreased from 29.910 to 29.900 in.Hg, the indicator in the capillary tube moved up by 1.85 cm. The length of the indicator column was fixed at 1 cm, and the volume of the downstream chamber was 11.3 cm<sup>3</sup>. The volume change per barometric pressure change was confirmed using the ideal gas equation; the indicator height change in the capillary tube due to a 0.0100 in.Hg pressure change was 1.84 cm. From the above calibration, when the permeation of a polymer film was ascertained by measuring the change in indicator column height, the volume change was recalculated for a constant barometric pressure. The permeability cell was first calibrated with known polymers, and their permeability coefficients were calculated according to the ASTM 1434 volumetric method. The pressure difference across the film was 300 kPa.

**Variable-Temperature <sup>1</sup>H Solid-State NMR Measurements.** The NMR experiments were performed with a Bruker MSL-200 spectrometer (4.7 T and 200 MHz for <sup>1</sup>H). The spin-lattice relaxation time in the rotating frame,  $T_{1\rho}$ , was measured at a temperature range from 140 to 400 K by analyzing the magnetization decay after <sup>1</sup>H 90°( $x$ )-spin-lock( $y$ )- $\tau$  pulse sequence, which provides useful information on molecular motions in the kilohertz frequency region. A <sup>1</sup>H 90° pulse width of 7.0  $\mu$ s was employed, and the repetition time for the net magnetization to be completely relaxed was 5–6  $T_1$ . Typically, 20–25 different  $\tau$  values were used, and FIDs were integrated in order to characterize the individual decay curves. Relaxation times were obtained as slopes of semilogarithmic plots of magnetization intensity vs  $\tau$ . Variable temperature was controlled by a Bruker control unit with accuracy of  $\pm 1$  °C.

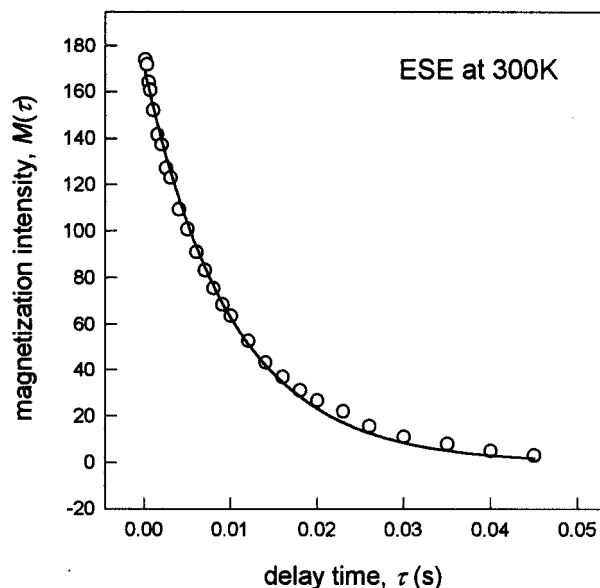
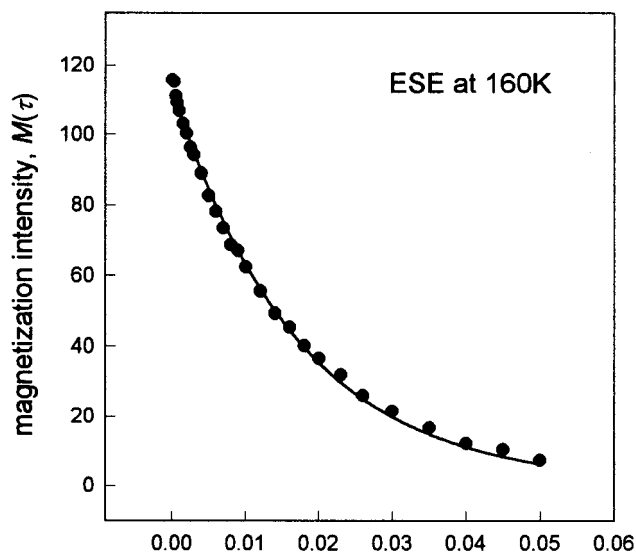
## Results and Discussion

Table 1 represents the glass transition temperatures, densities, and oxygen permeability coefficients for poly[oxy(ethylsulfonylmethyl)ethylene] (ESE), poly[oxy(propylsulfonylmethyl)ethylene] (*n*-PrSE), poly[oxy(butylsulfonylmethyl)ethylene] (BSE), and poly[oxy(pentylsulfonylmethyl)ethylene] (PeSE). ESE shows the oxygen barrier properties much better than many good barrier polymers, for example PET and Nylon 6, or comparable to commercial barrier polymers such as Barex, Lopac,

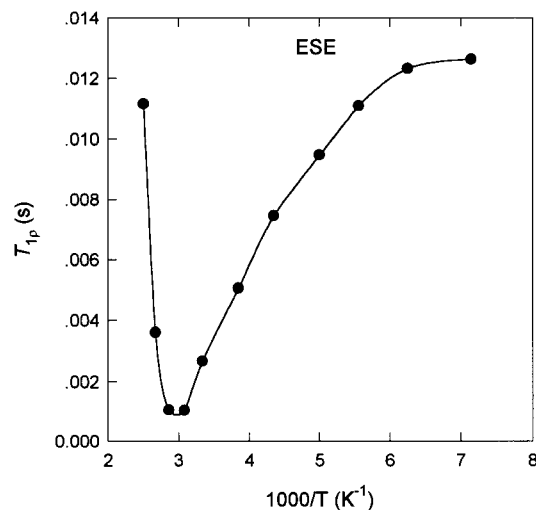
**Table 1.** Glass Transition Temperature ( $T_g$ ), Density, and Oxygen Permeability of (Alkylsulfonyl)methyl-Substituted Poly(oxyethylene)s

poly(oxyethylene)s	$T_g$ (°C)	density (g/cm <sup>3</sup> ) <sup>a</sup>	permeability coeff $\times 10^3$ [cm <sup>3</sup> (STP) cm/(cm <sup>2</sup> s Pa)]
ESE	57	1.361	0.0088
<i>n</i> -PrSE	43	1.292	0.22
BSE	37	1.265	0.40
PeSE	38	1.249	0.42

<sup>a</sup> Measured by neutral buoyancy method using a pycnometer: ref 18.

**Figure 1.** <sup>1</sup>H spin-lock relaxation of (ethylsulfonyl)methyl-substituted poly(oxyethylene) (ESE) at 160 K (●) and 300 K (○). Solid lines are nonlinear fits to a single-exponential decay.

and Saran.<sup>14,19</sup> As is shown in Scheme 1, the four oxyalkylene polymers have the same backbone repeat, oxyethylene, but differ in their alkyl side chains. As the side chain length increases, decreases in both density and  $T_g$  are the general trend, although the  $T_g$  of PeSE is slightly higher than that of BSE. However, the permeability coefficient of PeSE is slightly higher than that of BSE although the  $T_g$  of the former is slightly higher than that of the latter. The higher  $T_g$  of PeSE

**Figure 2.** Variation of <sup>1</sup>H  $T_{1\rho}$  of (ethylsulfonyl)methyl-substituted poly(oxyethylene) (ESE) as a function of temperature.

was attributable to the side chain crystallization and/or liquid crystallinity, which was described in detail in the previous paper.<sup>15</sup>

Figure 1 shows <sup>1</sup>H spin-lock magnetization decays as a function of delay time,  $\tau$ , for ESE at 160 and 300 K. The relaxation decays are characterized by an exponential function:

$$M(\tau) = M_0 \exp(-\tau/T_{1\rho}) \quad (1)$$

The decays were nonlinearly fit to within 95% confidence of the total signal by a single-exponential function from which the  $T_{1\rho}$  constants were derived. *n*-PrSE, BSE, and PeSE, although not shown here, also represent nonlinear relaxation decays similar to that of ESE which could be fit by a single-exponential function. The  $T_{1\rho}$  relaxation measurements were carried out over the temperature range 140–400 K, and their temperature dependence is shown in Figure 2. The variation of  $T_{1\rho}$  vs temperature for ESE has a minimum at  $\sim 330$  K with a value of  $1.05 \times 10^{-3}$  s, corresponding to  $\omega_1\tau_c = 0.5$ . Since the rf pulse frequency,  $\omega_1 = 55.6$  kHz, the correlation time,  $\tau_c$ , near 330 K is  $\sim 9 \times 10^{-6}$  s. The values of  $T_{1\rho}$  increase on both sides of the minimum, and the slope is smaller at the low-temperature side, i.e., the right side of the minimum. The temperature dependence of  $T_{1\rho}$  is characteristic of a single-activated process with correlation time,  $\tau_c$ , for which quantitative analyses by original Bloembergen–Purcell–Pound (BPP)<sup>12</sup> and Kubo–Tomita (KT)<sup>20</sup> provide relationships between the relaxation rate, internuclear distances, resonance frequency, and spectral density function of molecular motion (i.e., a measure of relative amount of motion). For protons, the principal mechanism of relaxation is through the time-dependent dipolar interactions, and the relaxation rates are given by

$$\frac{1}{T_{1\rho}} = \frac{3}{2}\gamma^4\hbar^2 I(I+1) \left[ \frac{1}{4} \mathcal{J}(2\omega_1) + \frac{5}{2} \mathcal{J}(2\omega_0) + \frac{1}{4} \mathcal{J}(2\omega_0) \right] \quad (2)$$

where  $\gamma$  is the proton magnetogyric ratio,  $\hbar$  is Planck's constant divided by  $2\pi$ ,  $r$  is the distance between coupled spins,  $I$  is the spin quantum number ( $=1/2$ ),  $\mathcal{J}(\omega)$  is the spectral density function at particular frequency,

$\omega_1$  is spin-lock field frequency, and  $\omega_0$  is Larmor frequency. Since  $J(\omega)$  is given by

$$J(2\omega_1) = \frac{24}{15r^6} \left[ \frac{\tau_c}{1 + 4\omega_1^2 \tau_c^2} \right] \quad (3)$$

$$J(\omega_0) = \frac{4}{15r^6} \left[ \frac{\tau_c}{1 + \omega_0^2 \tau_c^2} \right] \quad (4)$$

$$J(2\omega_0) = \frac{16}{15r^6} \left[ \frac{\tau_c}{1 + 4\omega_0^2 \tau_c^2} \right] \quad (5)$$

the relationship between relaxation and molecular motion is established as

$$\frac{1}{T_{1\rho}} = \frac{3}{10r^6} \gamma^4 \hbar^2 \left[ \frac{5/2\tau_c}{1 + \omega_0^2 \tau_c^2} + \frac{\tau_c}{1 + 4\omega_0^2 \tau_c^2} + \frac{3/2\tau_c}{1 + 4\omega_0^2 \tau_c^2} \right] \quad (6)$$

It is well-known that the relaxation behavior of polymeric materials follows an exponential relaxing process with a distribution of the relaxation times, whose broadness is dependent on the molecular environment. Unfortunately, rigorous theories have not yet been developed to fully describe such behavior concerning NMR relaxation. As a result, almost all the  $T_{1\rho}$  relaxation data have been treated with an empirical fitting function in order to represent the relaxation behavior and obtain the average local mobility. One of such empirical fitting functions with widespread acceptance is the very Bloembergen–Purcell–Pound (BPP) distribution function of the relaxation time. It is noteworthy that the distribution of relaxation behavior led by the distribution of local molecular environment can be estimated as follows.<sup>6,11,13</sup> As seen in the BPP eq 2, the  $T_{1\rho}$  relaxation is formulated by the summation of the spectral density function,  $J(\omega)$ ,

$$J(\omega) = \int_{-\infty}^{\infty} G(\tau) \exp(i\omega\tau) d\tau \quad (7)$$

$G(\tau)$  is an autocorrelation function and is assumed to be exponential,

$$G(\tau) = \exp(-|\tau|/\tau_c)^\beta \quad (8)$$

where  $\beta$  is the width parameter which is related to the distribution of the correlation time and hence the relaxation time contributed by the molecular environment. If  $G(\tau)$  is considered as arising from a superposition of exponentials, eq 8 may be written as

$$\exp(-|\tau|/\tau_c)^\beta = \int_0^\infty \exp(\tau/\tau_c) L(\tau) d\tau \quad (9)$$

where  $L(\tau)$  is a distribution function. If  $L(\tau)$  is determined, it will therefore give information about the broadness of the local molecular environment. Further insight into the  $T_{1\rho}$  vs temperature plot provides the determination of activation energies,  $E_a$ , which corresponds to the potential barrier for hindering the molecular motion. Recognizing that (a) the correlation time,  $\tau_c$ , is solely a function of the temperature through an Arrhenius law,  $\tau_c = \tau_0 \exp(E_a/RT)$ ,<sup>21</sup> where  $\tau_0$  is the

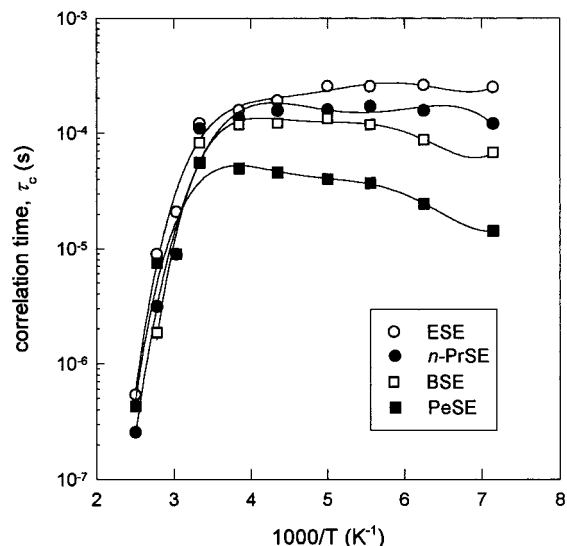


**Figure 3.** Temperature dependence of correlation times,  $\tau_c$ , for the four homologous series of poly(oxyethylene)s.

**Table 2. Comparison of Oxygen Permeability Coefficients, Correlation Times,  $\tau_c$ , at 160 and 300 K, and Activation Energies,  $E_a$ , for the Four (Alkylsulfonyl)methyl-Substituted Poly(oxyethylene)s**

poly(oxyethylene)s	permeability coeff $\times 10^3$ [cm <sup>3</sup> (STP) cm/(cm <sup>2</sup> s Pa)]	$\tau_c$ (s)		$E_a$ (kJ/mol)
		at 160 K	at 300 K	
ESE	0.0088	$2.11 \times 10^{-4}$	$1.22 \times 10^{-4}$	8.39
<i>n</i> -PrSE	0.22	$1.57 \times 10^{-4}$	$1.10 \times 10^{-4}$	7.29
BSE	0.40	$8.72 \times 10^{-5}$	$8.26 \times 10^{-5}$	6.98
PeSE	0.42	$2.47 \times 10^{-5}$	$5.60 \times 10^{-5}$	6.45

correlation time at infinite temperature (i.e., the pre-exponential factor) and  $R$  is the gas constant, and (b) at the lower-temperature side,  $T_{1\rho}$  is directly proportional to  $\tau_c$ , and hence  $T_{1\rho} \propto \exp(E_a/RT)$ , the  $E_a$  value can be estimated from the slope of low-temperature side of the minimum in logarithmic plot of  $T_{1\rho}$  vs  $1/T$ .

From eq 6, the correlation times,  $\tau_c$ 's, were extracted by nonlinear curve fitting of  $T_{1\rho}$  data at corresponding temperatures. The resulting  $\tau_c$ 's obtained for the four poly(oxyethylene)s as a function of temperature are displayed in Figure 3. As the  $\tau_c$  is a measure of molecular motion and the polymer with shorter  $\tau_c$  is in faster motion, the local chain mobility among the four poly(oxyethylene)s at temperatures ranging from 140 K to near room temperature ( $\sim 300$  K) is better in the order PeSE, BSE, *n*-PrSE, and ESE (also refer to Table 2). The ordering in  $\tau_c$  is in good agreement with the trend of an increase of the length in (alkylsulfonyl)methyl side chain and of the permeability. As the side chain length increases, neighboring chains are pushed further apart, increasing the free volume at a given temperature. This results in decreasing the hindrance to the chain backbone motions and, hence, enhancing the local chain motion.<sup>22–24</sup> Above the room temperatures over  $T_g$ 's of individual poly(oxyethylene)s in Figure 3, the correlation times began to change abruptly and decreased rapidly. In this region, the molecular motion is fast and the  $T_{1\rho}$  process may become ineffective, resulting in small dependence on temperatures. Thus, the data in this temperature range were included for the completeness of presentation, and they are not key to the rest of this study.



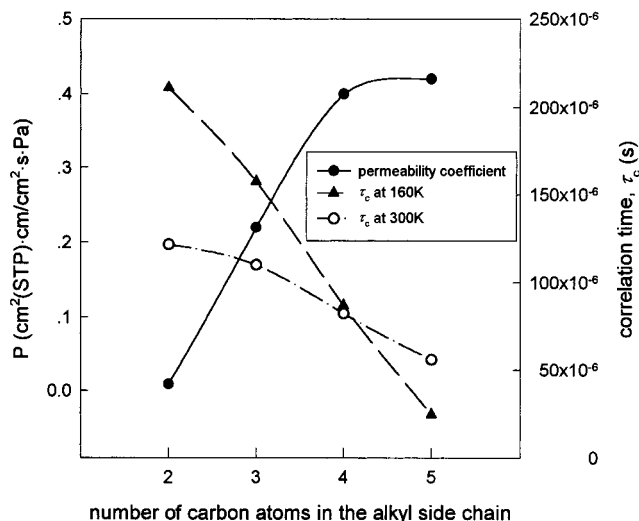


**Figure 4.** Relationship of correlation times,  $\tau_c$ , at two different temperatures with oxygen permeability coefficients of four poly(oxyethylene)s as a function of the number of carbons in the alkyl tail of side chain.

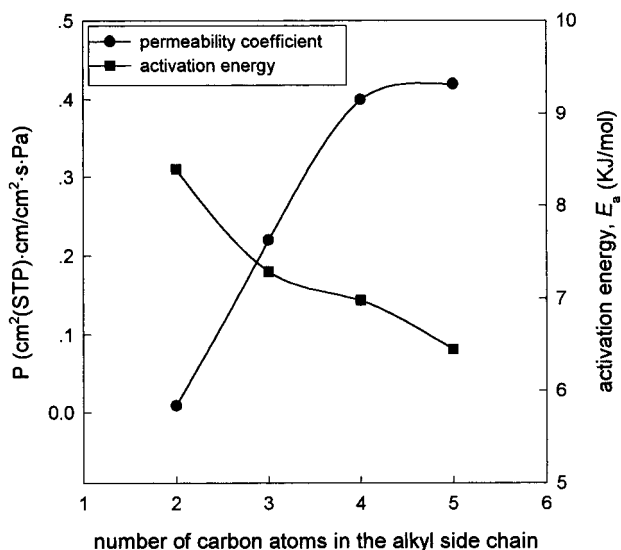


**Figure 5.** Relationship of activation energies,  $E_a$ , to oxygen permeability coefficients of four poly(oxyethylene)s as a function of the number of carbons in the alkyl tail of side chain.

Comparison of the correlation time values with reference to the oxygen permeability coefficient of the four poly(oxyethylene)s in conjunction with their structural variation is shown in Figure 4. There is an obvious correlation between the correlation time,  $\tau_c$ , and the permeability coefficient; the shorter the former the higher the latter, and vice versa. This indicates that the oxygen gas permeation across the poly(oxyethylene)s gets more elevated as the local chain motion became relatively more released with increasing side chain length in the order from ESE to PeSE. In contrast, restraining the polymer molecules retards the gas diffusion, resulting in improvement of barrier properties. Therefore, it is concluded that the local chain mobility plays a crucial role in governing the oxygen gas permeability of the poly(oxyethylene)s. This conclusion is also confirmed by the activation energies which characterize the energy barrier associated with the local molecular motion and hence  $\tau_c$ . As seen in Table 2 and Figure 5, the activation energies are ESE > *n*-PrSE > BSE > PeSE, and the corresponding gas permeabilities

are in the reverse trend, indicating higher resistance to the molecular motion from ESE to PeSE and, consequently, better barrier properties in that order.

## Conclusions

A correlation of the gas permeation with the local molecular motion was explored for the homologous series of poly(oxyethylene)s possessing structural variation; the structural variant was the difference in the length of (alkylsulfonyl)methyl side chains. The gas permeability measurements demonstrated that ESE, *n*-PrSE, BSE, and PeSE with increase in the side group length were in the order of lower to higher oxygen permeability coefficient. The proton spin–lattice relaxation times in the rotating frame,  $T_{1\rho}$ , characterized by variable-temperature pulsed wide-line  $^1\text{H}$  nuclear magnetic resonance (NMR) spectroscopy were used to determine the correlation times,  $\tau_c$ , which probe the local molecular motion of the four poly(oxyethylene)s. The longer correlation time of ESE was attributed to the shorter (alkylsulfonyl)methyl side chains, and vice versa for PeSE. The correlation times were in good correlation with the oxygen permeability coefficients; the longer  $\tau_c$ 's reflected the poly(oxyethylene) of less mobile chains which in turn made gas diffusion relatively more difficult, providing barrier properties, and vice versa for shorter  $\tau_c$ 's. The activation energies,  $E_a$ , also confirmed the correlation between  $\tau_c$  and oxygen permeability coefficient, showing the same trend as the  $\tau_c$ 's. Therefore, in addition to polarity, free volume, crystallinity, and orientation, the local molecular mobility determined by  $^1\text{H}$  solid-state NMR spectroscopy was another parameter to correlate and/or predict the gas permeability of polymers, especially of the homologous series of poly(oxyethylene)s such as ours.

**Acknowledgment.** The authors are grateful to the Korea Science and Engineering Foundation (KOSEF) for the support of this study through Hyperstructured Organic Materials Research Center (HOMRC).

## References and Notes

- (1) Pixton, M. R.; Paul, D. R. In *Polymeric Gas Separation Membranes*; Paul, D. R., Yampol'skii, Y. P., Eds.; CRC Press: Boca Raton, FL, 1994; Chapter 3.
- (2) Koros, W. J., Ed. *Barrier Polymers and Structures*; American Chemical Society: Washington, DC, 1990.
- (3) Houde, A. Y.; Kulkarni, S. S.; Jharul, U. K.; Charati, S. G.; Kulkarni, M. G. *J. Membr. Sci.* **1994**, *103*, 167.
- (4) Hirayama, Y.; Yoshinaga, T.; Ninomiya, K.; Sakakibara, T.; Tamari, T. *J. Membr. Sci.* **1996**, *111*, 183.
- (5) Paul, W.; Weber, H.; Binder, K. *Ann. Phys. (Leipzig)* **1998**, *7*, 554.
- (6) McBrierty, V. J.; Packer, K. J. *Nuclear Magnetic Resonance in Solid Polymers*; Cambridge University Press: Cambridge, 1993.
- (7) McCrum, N. G.; Read, B. E.; Williams, G. *Anelastic and Dielectric Effects in Polymeric Solids*; John Wiley & Sons: New York, 1976.
- (8) Bailey, R. T.; North, A. M.; Pethrick, R. A. In *Molecular Motion in High Polymers*; Clarendon Press: Oxford, 1981; Chapter 10.
- (9) Hartmann, S. R.; Hahn, E. L. *Phys. Rev.* **1962**, *128*, 2042.
- (10) Schaefer, J.; Stejskal, E. O. *J. Chem. Soc.* **1976**, *98*, 1032.
- (11) Ando, I. In *Solid NMR of Polymers*; Sainendefuku: Tokyo, 1994; Chapter 4 (in Japanese).
- (12) Bloembergen, N.; Purcell, E. M.; Pound, R. U. *Phys. Rev.* **1948**, *73*, 679.
- (13) Bruch, M. D., Ed. *NMR Spectroscopy Techniques*; Marcel Dekker: New York, 1996.
- (14) Lee, J.-C.; Litt, M. H.; Rogers, C. E. *J. Polym. Sci., Polym. Phys. Ed.* **1998**, *36*, 75.

- (15) Lee, J.-C.; Litt, M. H.; Rogers, C. E. *Macromolecules* **1997**, *30*, 3776.
- (16) *Annual Book of ASTM Standard*, D 1434, Sec. 15; Vol. 15.09, 1991.
- (17) Ashely, R. J. In *Polymer Permeability*; Elsevier: London, 1985; p 269.
- (18) Runt, J. P. In *Encyclopedia of Polymer Science and Engineering*; Mark, H., Bikales, N. M., Overberger, C. E., Menges, G., Eds.; John Wiley & Sons: New York, 1986; Vol. 4, p 458.
- (19) Litt, M. H. *J. Rheol.* **1986**, *30*, 853.
- (20) Kubo, R.; Tomita, K. *J. Phys. Soc. Jpn.* **1954**, *9*, 888.
- (21) Jones, A. A. In *High-Resolution NMR Spectroscopy of Synthetic Polymers in Bulk*; Komoroski, R. A., Ed.; VCH: Deerfield Beach, 1986; Chapter 7.
- (22) Rogers, S. S.; Mandelkern, L. *J. Phys. Chem.* **1957**, *61*, 985.
- (23) Hayes, R. A. *J. Appl. Polym. Sci.* **1961**, *15*, 318.
- (24) Wesslin, B.; Lenz, R. W.; MacKnight, W. J.; Karaz, F. E. *Macromolecules* **1971**, *4*, 24.

MA991417W